ELSEVIER

Polymer 41 (2000) 1817–1826

polymer

On the mechanical properties of co-continuous polymer blends: experimental and modelling

Harm Veenstra[a,*], Paul C.J. Verkooijen[a], Barbara J.J. van Lent[a], Jaap van Dam[a], Albertus P. de Boer[a], Abe Posthuma H.J. Nijhof[b]

[a]*Department of Polymer Technology, Faculty of Chemical Technology and Materials Science, Delft University of Technology, Julianalaan 136, 2628 BL Delft, The Netherlands*

[b]*Department of Engineering Mechanics, Subfaculty of Mechanical Engineering and Marine Technology, Delft University of Technology, Mekelweg 2, 2628 CD Delft, The Netherlands*

Received 20 October 1998; received in revised form 9 February 1999; accepted 5 May 1999

Abstract

Mechanical properties of polymer blends with co-continuous morphologies were measured and compared to the properties of blends of the same polymers with a droplet/matrix morphology. For this purpose, poly(ether–ester)/PS and SEBS/PP blends were prepared with both morphologies, which was facilitated by the rheological properties of the block copolymers. The elastic moduli of co-continuous blends were significantly higher than the moduli of the dispersed blends, but no significant difference in tensile or impact strength was found when co-continuous blends were compared to blends with a droplet/matrix morphology. A model was proposed depicting the basic element of co-continuous structures as three orthogonal bars of one component embedded in a unit cube where the remaining volume was occupied by the other component. This model was shown to predict the moduli of polymer blends with co-continuous morphologies over the complete composition range.

Keywords: Co-continuous morphology; Blends; Mechanical properties

1. Introduction

An elegant method to obtain new materials is blending of thermoplastic polymers. The properties of these polymer blends are to a large extent determined by the morphology, i.e. the size, shape and distribution of the components [1]. Factors governing the morphology are composition, interfacial tension, processing conditions and rheological properties of the components. In general, polymer blend morphologies can be divided into three classes, i.e. dispersed, stratified and co-continuous morphologies. Dispersions of droplets of the minor phase in a matrix of the major phase are most common. These types of blends are often used in rubber modification of brittle polymers [1–4]. The minor phase can also be dispersed as fibers, for example in self-reinforcing polymer blends [5–7]. In these kinds of blends the properties are mainly improved in the direction of the fibers. In literature many papers are dedicated to the mechanical properties of polymer blends with dispersed morphologies. Much less is known about the mechanical properties of co-continuous morphologies despite the interesting feature that both components, in all directions, can fully contribute to the properties of the blend.

It was long believed that co-continuous morphologies are mainly formed around the point of phase inversion. We have shown that co-continuous morphologies are not formed at a single volume fraction, such as a point of phase inversion, but rather over a range of volume fractions [8–12]. This range of volume fractions strongly depends on the processing conditions and the rheological properties of the components [8,11,12]. In particular, in blends with thermoplastic elastomers (TPEs) co-continuous morphologies can be obtained over a wide composition range [9–12]. In an earlier paper [11], the formation of such a wide composition range was related to the specific rheological properties of TPEs. TPEs are block copolymers where the blocks are phase separated into micro-domains. These phase-separated domains, also called physical crosslinks, are responsible for the unique (rheological) properties of TPEs. A detailed knowledge of the rheological and thermal properties of TPEs, related to their specific microstructure, enables us to control the formation [11,12] and stability [13] of co-continuous morphologies. A proper choice of processing conditions results in a composition range of co-continuous

* Corresponding author. Tel.: +31-15-2781828; fax: +31-15-2787415.

0032-3861/00/$ - see front matter
PII: S0032-3861(99)00337-7

Table 1
Blend components, temperature of processing (T_p) and resulting range of co-continuity for all systems after processing and compression moulding

System	Components	T_p (°C)	Range of co-continuity
Ia	PS/poly(ether–ester)	230	50–60 vol.% PS
Ib	PS/poly(ether–ester)	200	30–60 vol.% PS
IIa	PP/SEBS	250	50–60 vol.% PP
IIb	PP/SEBS	190	40–80 vol.% PP

morphologies that is either wide or small. Therefore, at a single volume fraction, co-continuous as well as dispersed morphologies can be obtained. This gives us the opportunity to compare the mechanical properties of polymer blends with a dispersed morphology to the mechanical properties of the same blend with a co-continuous morphology.

The literature that is available about the mechanical properties of co-continuous polymer blends, experimental [14–23] as well as modelling [21,24,25], is scarce. There are a few reports [14,15] showing an increase in impact strength in the case of co-continuity, but some other reports show no effect of co-continuity [16]. Other authors [17–19] compared measured elastic moduli to the Davies model [24], which is mostly used for co-continuous morphologies. When the fit was reasonable they concluded that the blend must be co-continuous. Without knowing the exact morphology this can lead to mistakes because deviations from the Davies model are also found [20,22]. Earlier work in our laboratory [22] has shown that co-continuous morphologies are characterized by high values for the tensile modulus exceeding the theoretical predictions. It can be concluded that the influence of co-continuity on the mechanical properties of polymer blends requires further investigation.

The objective of this paper is to trace the influence of co-continuity on the mechanical properties of polymer blends. Therefore, a number of blends has been studied with either a small or a wide composition range of co-continuity. The mechanical properties of co-continuous blends will be compared to the mechanical properties of blends with dispersed morphologies. The mechanical properties as function of the composition will be related to the change in morphology, and a model will be proposed that can describe the moduli of co-continuous polymer blends.

2. Experimental

2.1. Materials

The polymers that were used are polystyrene (PS Hostyrene N7000; Shell), polypropylene (PP Stamylan P13E10; DSM), styrene/(ethylene–butylene) based block copolymer (SEBS Kraton G1657; Shell) and poly(ether–ester) multiblock copolymer (Arnitel EM400; DSM). The SEBS G1657 has a styrene to rubber ratio of 13/87 wt.%, and consists of 65% triblock and 35% diblock. Arnitel EM400 is a poly(ether–ester) multiblock copolymer, consisting of 40 wt.% hard, crystalline poly(tetra methylene terephthalate) segments and 60 wt.% soft, amorphous poly(tetra methylene oxyde) segments. The melting and crystallization characteristics of this polymer as well as the rheological properties are described in Ref. [26]. Blends are prepared in the composition range 10–90 vol.% and will be divided into four different systems. Systems Ia and Ib are blends of PS and poly(ether–ester), and systems IIa and IIb are blends of PP and SEBS. A proper choice of the processing conditions will result in a small (Ia and IIa) or wide (Ib and IIb) composition range of co-continuous morphologies [11–13] (Table 1).

2.2. Processing

All blends, except for system Ib, were prepared on a 20 mm Collin laboratory extruder equipped with a transport screw, and a static mixer in series with the extruder containing 10 Ross ISG 15 mm diameter mixing elements. Each element contains four channels with a radius of 0.135 cm. The average shear rate in the channels was estimated to be $30\ s^{-1}$. The extruded strands were quenched in water. Systems Ia, IIa and IIb were processed at 230, 250 and 190°C, respectively. System Ib was prepared at 200°C on a two-roll mill (Schwabentahn) with roll speeds of 0.136 and $0.163\ m\ s^{-1}$. The gap between the two rolls was 1.10 mm resulting in an average shear rate of $150\ s^{-1}$. The blends were scraped off the mill after 12 min and directly quenched in water at room temperature.

Samples for mechanical testing were prepared by compression moulding. Systems Ia and Ib were compression moulded at 210°C for 7 min, system IIa was prepared in 5 min at 250°C, and system IIb in 2.5 min at 190°C. Samples of the pure components were prepared in the same way as the blends, i.e the same processing and compression moulding procedure, in order to check if the processing procedure had any influence on the mechanical properties of the pure components.

2.3. Morphology

The morphology was characterized by means of a Philips XL20 scanning electron microscope (SEM) and by extraction experiments. One component of the blend was extracted with a selective solvent, i.e. 2-butanone to extract PS and iso-octane to extract SEBS. The combination of extraction experiments and SEM is essential in determining whether a blend is co-continuous or not. A blend is only considered fully co-continuous if 100% of one of the components can be extracted and the remaining piece is still self-supporting.

2.4. Mechanical testing

Tensile measurements were performed in accordance

Table 2
Percentage of PS (systems Ia and Ib) or SEBS (systems IIa and IIb) extracted from blends that were processed and compression moulded into tensile bars. The samples indicated with (–) are no longer self-supporting after extraction

Volume fraction	System Ia (PS/poly(ether–ester))	System Ib (PS/poly(ether–ester))	System IIa (PP/SEBS)	System IIb (PP/SEBS)
10/90	25	23	–	98
20/80	15	20	–	100
30/70	16	90	–	98
40/60	83	100	–	98
50/50	99	100	100	99
60/40	100	100	99	100
70/30	–	–	87	100
80/20	–	–	36	91
90/10	–	–	2	11

with ISO R527 at room temperature on an Instron tensile tester with a crosshead speed of 10 mm min^{-1}. All samples were tested until an elongation of 200% was reached (the elongation was limited by the tensile tester). The Young's modulus (E_y) is determined from the initial slope of the stress–strain curve.

A Perkin Elmer DMA 7e in three point bending mode was used to determine the storage modulus (E') as a function of temperature. The samples ($15 \times 4 \times 1$ mm^3) were heated with 5°C min^{-1} and measured at a frequency of 1 Hz.

Impact tests were performed on a Zwick pendulum apparatus equipped with 1.0–5.5 J hammers. All samples ($60 \times 10 \times 4$ mm^3) were notched on an automatic notching machine (Ceast).

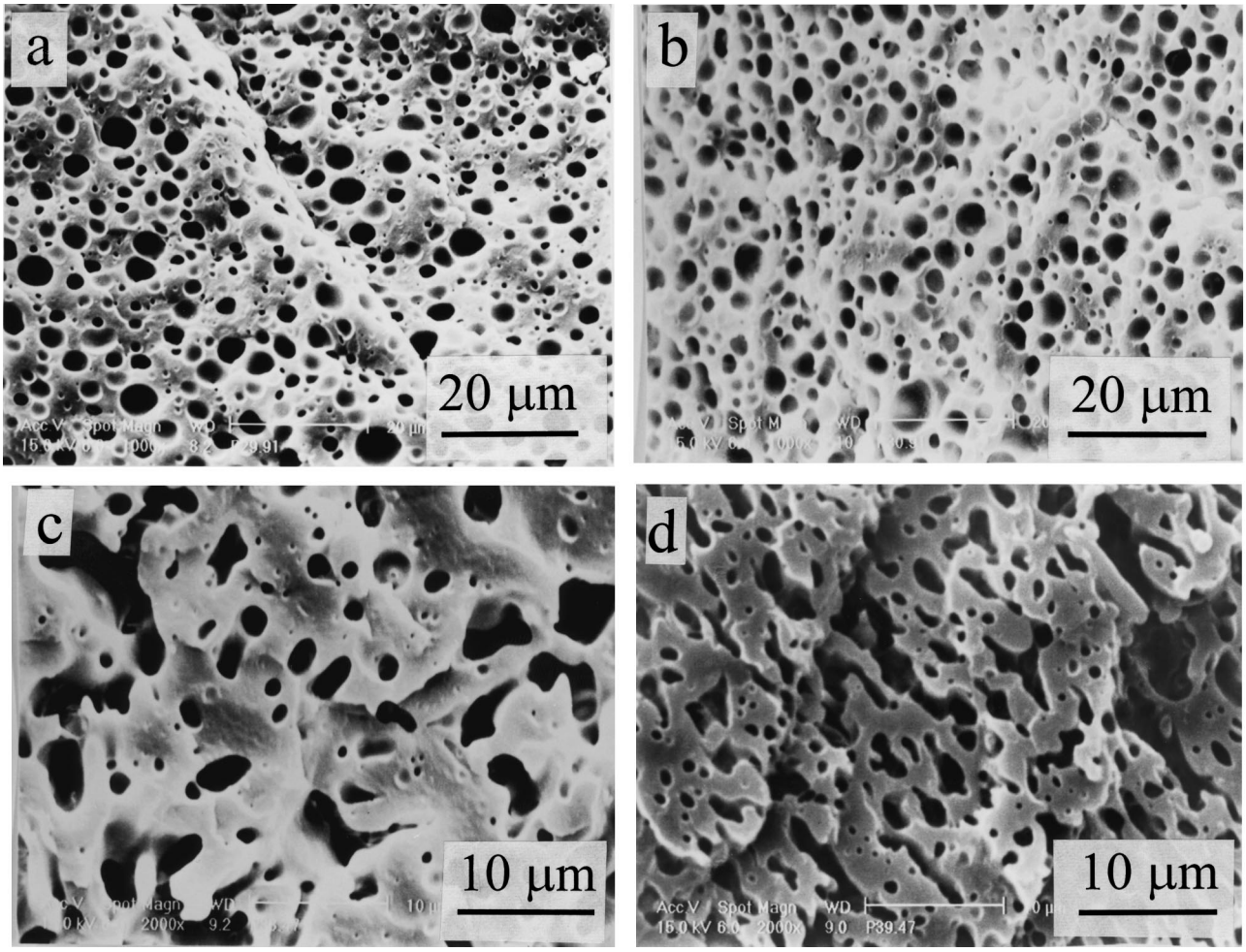

Fig. 1. SEM micrographs of PS/poly(ether–ester) blends of systems Ia (a and b) and Ib (c and d) with 30 and 40 vol.% PS.

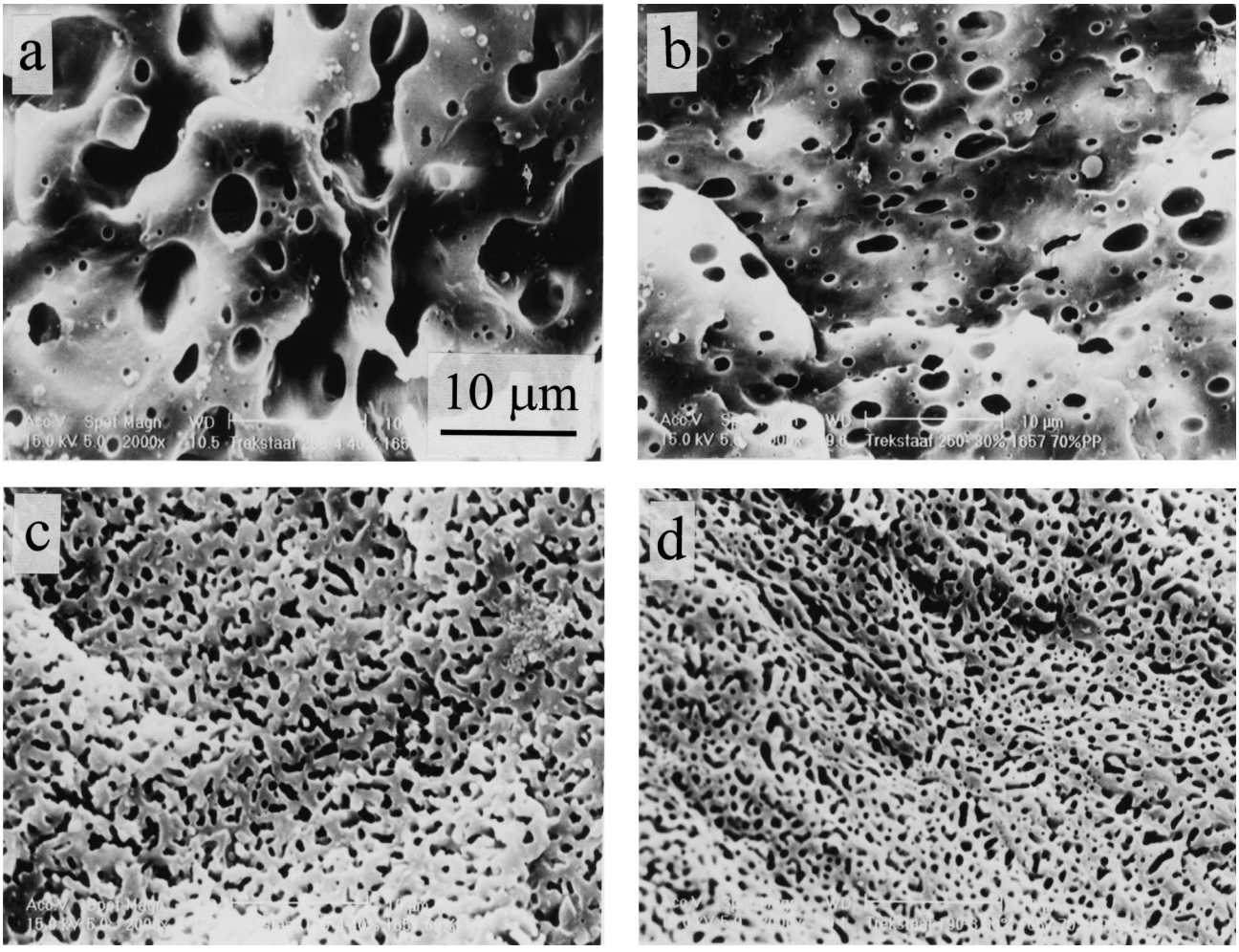

Fig. 2. SEM micrographs of PP/SEBS blends of systems IIa (a and b) and IIb (c and d) with 60 and 70 vol.% PP.

3. Results and discussion

3.1. Morphology

The results of the extraction experiments on samples taken from tensile bars, showing the percentage PS extracted for systems Ia and Ib, and the percentage SEBS extracted for systems IIa and IIb are given in Table 2. The blends that were no longer self-supporting after one phase were extracted, and are indicated with a bar. To determine the co-continuity a combination of extraction experiments and SEM is essential.

The blends of systems Ia and Ib with 30 and 40 vol.% PS are depicted in Fig. 1. The SEM micrographs show the poly(ether–ester) matrix (grey sections) that is left after the PS phase was extracted (dark sections). The results from the extraction experiments and the SEM micrographs clearly show that by adequate processing [11–13], either a droplet/matrix morphology (Fig. 1(a) and (b)) or a co-continuous one (Fig. 1(c) and (d)), at a certain composition, can be obtained. The result is that system Ia shows co-continuous morphologies, after processing and compression moulding, over a small composition range (50–60 vol.% PS) and system Ib over a broader range of compositions (30–60 vol.% PS). All other compositions of systems Ia and Ib show droplet/matrix morphologies. The phase sizes of all blends are in the same order of magnitude, i.e. the droplets show diameters around a micron and the phase sizes of the co-continuous blends are a few microns.

The blends of systems IIa and IIb, that were processed and compression moulded, with 60 and 70 vol.% PP are depicted in Fig. 2. The SEM micrographs show the PP matrix (grey sections) that is left after the SEBS phase was extracted (dark sections). SEM analysis together with the extraction results clearly show that adequate processing [11–13] of the PP/SEBS systems results in a small composition range of co-continuous morphologies (50–60 vol.% PP) for system IIa, and a wide composition range (40–80 vol.% PP) for system IIb. All other compositions of system IIa, as well as the 90 vol.% PP blend of system IIb, show dispersed morphologies. Although the samples of system IIb with 10–30 vol.% PP do not fall apart upon extraction, no clear morphology could be detected with SEM analysis because the samples collapse upon solvent

Table 3
Impact strength (kJ/m^2) of all systems. The samples that did not break upon testing are indicated with (n.b.). The results for co-continuous blends are in italic

Volume fraction	System Ia (PS/ poly(ether–ester))	System Ib (PS/ poly(ether–ester))	System IIa (PP/SEBS)	System Iib (PP/SEBS)
0/100	n.b.	n.b.	n.b.	n.b.
10/90	n.b.	n.b.	n.b.	n.b.
20/80	n.b.	n.b.	n.b.	n.b.
30/70	8.2 ± 0.3	*5.4 ± 0.2*	n.b.	n.b.
40/60	4.2 ± 0.4	*5.3 ± 1.3*	n.b.	n.b.
50/50	*6.2 ± 2.3*	*3.2 ± 0.5*	n.b.	n.b.
60/40	*4.2 ± 0.7*	*2.9 ± 0.5*	n.b.	n.b.
70/30	2.7 ± 0.6	1.8 ± 1.0	n.b.	n.b.
80/20	1.7 ± 0.2	1.9 ± 0.2	40 ± 2.7	*40 ± 1.4*
90/10	1.5 ± 0.2	1.4 ± 0.3	24 ± 1.5	25 ± 2.1
100/0	1.3 ± 0.2	1.3 ± 0.2	4.1 ± 0.6	4.1 ± 0.6

evaporation. Most probably some transition morphology in between a co-continuous and a dispersed morphology was formed. The phase sizes of systems IIa and IIb do not differ too much. Most blends show droplet diameters or co-continuous strands of around 0.5 micron. Only the dimensions of the 50 and 60 vol.% PP blends of system IIa are somewhat larger (2–3 micron), which can be explained by a coarsening of co-continuous morphologies with time [13].

3.2. Impact properties

The results of the impact tests that were performed on a Zwick pendulum apparatus are shown in Table 3. It becomes clear from the results of systems Ia and Ib that increasing the amount of PS reduces the impact strength of the PS/poly(ether–ester) blends. No significant difference was found between the impact properties of co-continuous and dispersed polymer blends, considering the relative large errors associated with these kind of experiments.

The samples of the PP/SEBS blends (systems IIa and IIb) did not break at all until the amount of PP was increased to 80 vol.%. Further increase of the amount of PP reduced the impact strength. Also, in this case, the impact strength values that were found are the same for both systems, despite the differences in morphology.

3.3. Tensile properties

The Young's moduli (E_y) for systems Ia and Ib, as obtained from the initial slope of the stress–strain curves, are plotted as a function of volume fraction PS in Fig. 3(a). It becomes clear that at low volume fractions of PS, the measured values for E_y are close to the series model ($E^{-1} = \phi_1/E_1 + \phi_2/E_2$). The moduli show a sharp increase when PS becomes continuous throughout the sample. At

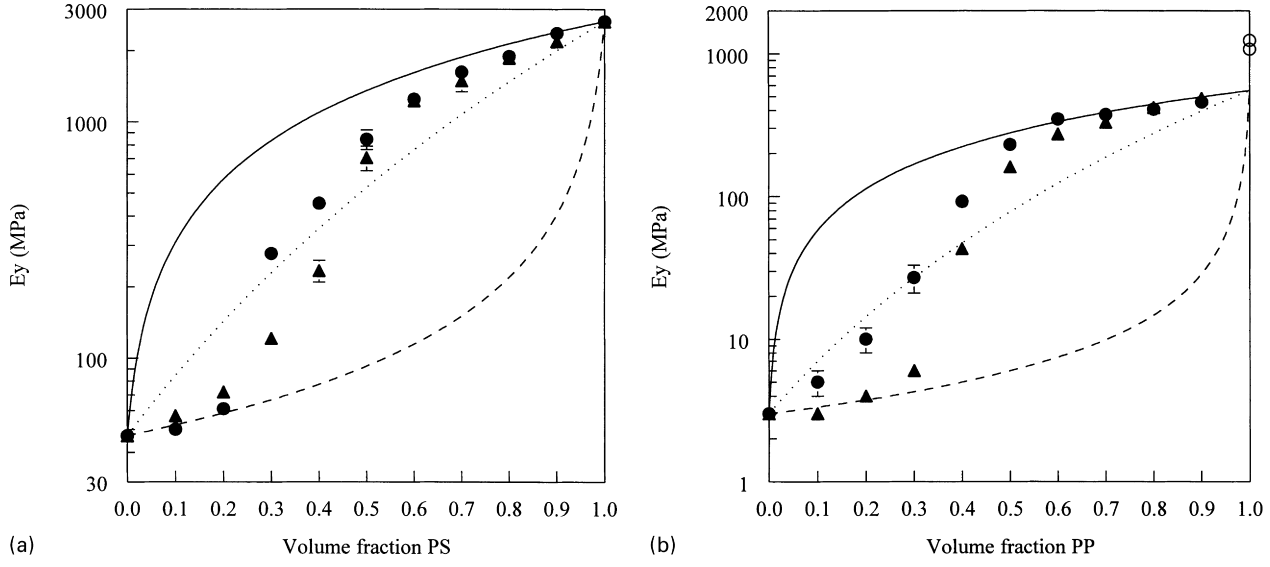

Fig. 3. (a) Young's moduli for the PS/poly(ether–ester) systems Ia (▲) and Ib (●) as a function of volume fraction PS; (b) Young's moduli for the PP/SEBS systems IIa (▲) and IIb (●) as a function of volume fraction PP (when the error bars are not visible they are smaller than the marker). The experimental values are compared with the parallel (—), series (– – –) and Davies (……) model.

Table 4
Maximum tensile stress (σ_t) of all systems determined on a Instron tensile tester. The samples for which no maximum tensile stress could be determined within the limit of 200% elongation are designated with (–). The results for co-continuous blends are in italic

Volume fraction	System Ia (PS/ poly(ether–ester))	System Ib (PS/ poly(ether–ester))	System IIa (PP/SEBS)	System IIb (PP/SEBS)
0/100	–	–	–	–
10/90	–	–	–	–
20/80	–	–	–	–
30/70	–	*9.1*	–	–
40/60	11.8	*10.3*	–	–
50/50	*15.2*	*12.8*	–	–
60/40	*20.0*	*18.8*	*12.3*	*14.6*
70/30	24.3	18.2	16.2	*16.6*
80/20	31.8	24.8	20.6	*20.8*
90/10	35.4	31.0	24.2	26.7
100/0	42.1	41.3	28.4	28.6

high volume fractions of PS, the moduli are somewhat lower than those of the parallel model ($E = \phi_1 E_1 + \phi_2 E_2$). When the moduli of the co-continuous blends are compared to those of the dispersed morphologies (with the same volume fractions), it becomes evident that at low volume fractions of PS the co-continuous blends show a higher value for the modulus than the dispersed blends. Apparently, PS contributes more to the modulus of the blend when it is continuous than when it is dispersed in the poly(ether–ester) matrix which must be related to a more effective stress transfer in the case of co-continuity. At higher volume fractions of PS, the difference in modulus related to the difference in morphology diminishes. Fig. 3(a) also shows that the Young's moduli of co-continuous blends cannot be described by Davies' model [24], i.e. all experimental values are higher than that predicted by the model ($E^{1/5} = \phi_1 E_1^{1/5} + \phi_2 E_2^{1/5}$). It was shown in an earlier paper by our group [22] that the Young's moduli of co-continuous blends could not be predicted by the models available for co-continuity.

The different processing and compression moulding conditions did not influence the modulus values of the pure components, thereby implying that the moduli of the blends as described above are related to the morphology and composition only.

The Young's moduli for systems IIa and IIb as a function of volume fraction PP are shown in Fig. 3(b). The same trends are found for the PP/SEBS systems as those for systems Ia and Ib, i.e. the modulus sharply increases when PP becomes continuous and the values for droplet/matrix blends are close to the series and the parallel models at low and high volume fraction PP, respectively. It is also evident that the co-continuous blends show a much higher value for the Young's modulus than the dispersed blends (at the same volume fraction). Also, in the range of transition morphologies (10–30 vol.% PP, system IIb), an increase in the Young's modulus is found when compared to the blends with a droplet/matrix morphology. The experimental values for the Young's moduli of the co-continuous blends are again higher than those predicted by the Davies model.

The predictions according to the series, parallel and Davies models for the systems IIa and IIb were calculated using the extrapolated values for the Young's modulus of pure PP. This was done because addition of small amounts of SEBS causes a strong reduction of the modulus, e.g. adding 10% of SEBS results in a drop of the modulus to halve the value of the modulus of pure PP (indicated in Fig. 3(b) by an open circle). Other authors [20,27] too have found a similar large reduction in modulus. This strange behaviour cannot be explained by mixing on a molecular scale as no changes occur in melting point, melting enthalpy and glass transition temperatures [12]. Some authors [28], however, have shown that at the PP–SEBS interface some interdiffusion occurs. Although a proper explanation for the large reduction in modulus cannot be given, it does not influence the conclusions which can be drawn from Fig. 3(b), i.e. the effects of morphology on the moduli of polymer blends.

The maximum tensile stress (σ_t), i.e. the yield stress for samples that yielded, and the stress at break for samples that showed a brittle fracture, of all blends are shown in Table 4. When PS is dispersed in the poly(ether–ester) matrix the samples simply do not break within the limit of 200% elongation, but when PS becomes continuous the maximum elongation is sharply reduced. No significant differences are found for the maximum tensile stresses. No samples of systems IIa and IIb break within an elongation of 200%. Also, for systems IIa and IIb no significant differences in maximum tensile stress are found when co-continuous blends are compared to the blends with a dispersed morphology.

3.4. Storage modulus

The storage moduli (E') of systems Ia and Ib, determined at room temperature, as a function of volume fraction of PS are plotted in Fig. 4(a). It is evident that the storage moduli

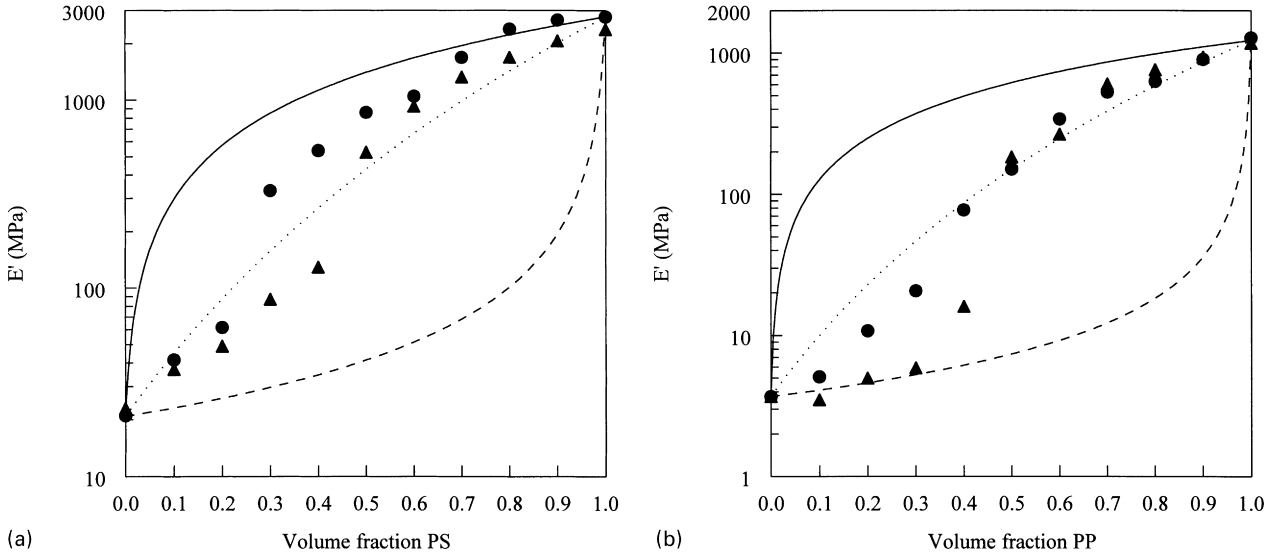

Fig. 4. (a) Storage moduli for the PS/poly(ether–ester) systems Ia (▲) and Ib (●), obtained at room temperature, as a function of volume fraction PS; (b) Storage moduli for the PP/SEBS systems IIa (▲) and IIb (●), obtained at room temperature, as a function of volume fraction PP. The experimental values are compared with the parallel (—), series (– – –) and Davies (……) model.

show the same behaviour as is found for the Young's moduli. The moduli of the co-continuous blends are again higher than the moduli of blends with dispersed morphologies and a substantial increase in modulus is found when PS becomes continuous.

The storage moduli (E') of systems IIa and IIb, determined at room temperature, as a function of volume fraction of PP are plotted in Fig. 4(b). Again the same behaviour is found as was described above.

In Fig. 5, the storage modulus of blends with 40 vol.% PP is plotted as a function of temperature for systems IIa and IIb. For comparison, the storage moduli of the pure components are also plotted. It is evident that at all temperatures higher than the glass transition of SEBS, the modulus of the co-continuous blend is higher than that of the blend with a dispersed morphology, i.e. over a wide temperature range co-continuous blends are more effective in providing stiffness and strength to the material than the dispersed blends.

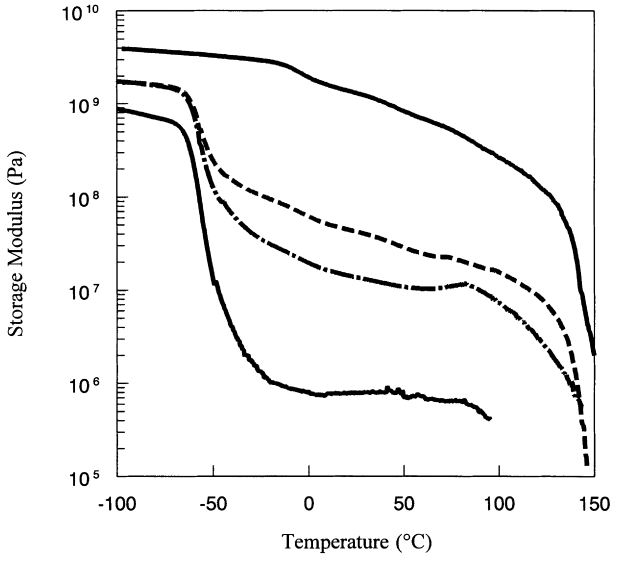

Fig. 5. Storage modulus of PP (–), SEBS (-) and blends with 40 vol.% PP as a function of temperature for system IIa (- -) and IIb (– –).

3.5. Modelling

Figs. 3 and 4 make clear that co-continuous blends show higher experimental values for the moduli than is predicted by the Davies model. It was also shown in an earlier paper by our group [22] that the Young's moduli of co-continuous blends could not be predicted by any model available for co-continuity. These models cannot predict the moduli of co-continuous blends because they do not incorporate the dual phase interconnectivity which is typical for co-continuous blends, except Kolařík's model. Therefore, a model is developed that incorporates this dual phase interconnectivity to obtain a better description of co-continuous polymer blends.

A combination of parallel and series elements as proposed by Takayanagi [29] for two-dimensional and Barentsen [30] for three-dimensional geometries can be used to describe droplet/matrix blends. Barentsen's model can either be described as a series model of parallel parts (Fig. 6(a) and Eq. (1)) or a parallel model of serial linked parts (Fig. 6(b) and Eq. (2)). The unit cubes, as shown in Fig. 6(a) and (b), can be used for modelling of polymer blends with a droplet/matrix morphology when the dispersed particles are evenly distributed in the matrix.

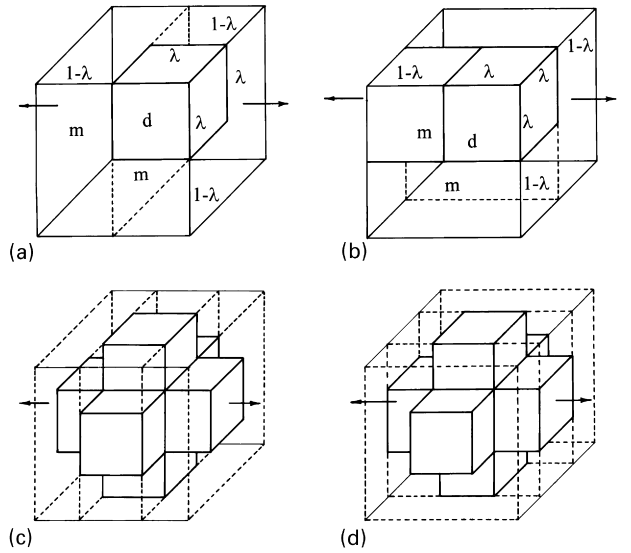

Fig. 6. Three-dimensional models for the calculation of the moduli of dispersed polymer blends (a and b) and co-continuous polymer blends (c and d).

$$E_a = E_m \frac{\lambda^2 E_d + (1-\lambda^2)E_m}{(1-\lambda)\lambda^2 E_d + (1-\lambda^2+\lambda^3)E_m} \quad (1)$$

$$E_b = (1-\lambda^2)E_m + \frac{\lambda^2 E_m E_d}{\lambda E_m + (1-\lambda)E_d}. \quad (2)$$

The modulus of the blend (E_a or E_b) is expressed as a function of volume fraction ($\phi_d = 1 - \phi_m = \lambda^3$), modulus of the dispersed phase (E_d) and modulus of the matrix (E_m).

In a co-continuous morphology, the dispersed phase does not consist of separate particles in the matrix phase, but is interconnected and forms elongated domains, which extend throughout the matrix. To visualize co-continuity, a model is proposed that consists of three orthogonal bars of polymer 1 embedded in a unit cube where the remaining volume is occupied by component 2. Repeating this unit cube in 3D shows that component 2 has the same framework as component 2, i.e. both the components are interconnected. In a similar manner, as Barentsen did, relations for a series model of parallel parts (Fig. 6(c) and Eq. (3)) and for a parallel model of serial-linked parts (Fig. 6(d) and Eq. (4)) can be derived [31] as:

$$E_c \frac{(a^4 + 2a^3b)E_1^2 + 2(a^3b + 3a^2b^2 + ab^3)E_1E_2 + (2ab^3 + b^4)E_2^2}{(a^3 + a^2b + 2ab^2)E_1 + (2a^2b + ab^2 + b^3)E_2} \quad (3)$$

$$E_d = \frac{a^2bE_1^2 + (a^3 + 2ab + b^3)E_1E_2 + ab^2E_2^2}{bE_1 + aE_2} \quad (4)$$

where a is related to the volume fraction of component 1 by $3a^2 - 2a^3 = \phi_1$ and b is related to the volume fraction of component 2 by $b = 1 - a$.

The model for co-continuity as shown in Fig. 6(d) and Eq. (4) is comparable to the COS model proposed by Kolařík [25], but in addition to the parallel model of serial-linked parts we also introduce a series model of parallel-linked parts for co-continuity. We, therefore, have the opportunity to distinguish between the different influences of a weak and a stiff component on the modulus of the blend.

First, a dispersion of the stiff component in a matrix of the weak component will be considered. In the model as depicted in Fig. 6(a), the dispersion will force a large part of the weak matrix (perpendicular to the direction of force) to the same elongation as the stiff dispersion. However, in reality, because the matrix is weak, the influence of the stiff dispersion in the direction perpendicular to the force direction will be limited. Therefore, this model seems inappropriate. In the model as depicted in Fig. 6(b), the stiff dispersion forces the part of the weak matrix that is coupled in series with it to an elongation that is much longer than the elongation of the rest of the matrix. This is in agreement with reality because in real blends the weak matrix will deform most at the interface between the stiff droplets and the weak matrix (relative high strain gradients in the weak matrix do not cost so much energy). Therefore, the model as depicted in Fig. 6(b) is more appropriate when the weak component dominates.

In the case of a weak dispersion in a stiff matrix the model given in Fig. 6(b) cannot be used. In this model, there is a difference in elongation between the stiff matrix parts that are parallel-connected, but in practice the matrix will have the same elongation throughout the whole sample (The strain gradient between the parallel parts is small). The model as depicted in Fig. 6(a) seems, therefore, more appropriate when the stiff component dominates. The same arguments can be used for the parallel model of serial-linked parts (Fig. 6(d) and Eq. (4)) and the series model of parallel-linked parts (Fig. 6(c) and Eq. (3)) that were derived for co-continuous blends.

This means that at volume fractions (0–50 vol.%) where the stiff component is the minor phase Eqs. (2) and (4) must be used. When the stiff component dominates (50–100 vol.%), Eqs. (1) and (3) must be used. The complete composition range, from 100% of the first component to 100% of the second component, can now be modelled if the morphology is known. In the intermediate regions, i.e. from distinct droplet/matrix morphologies to full co-continuous morphologies an interpolation between the two models is used. Around 50 vol.% (±5%), an average of the two co-continuous models is used and also between the three co-continuity regions we used interpolations. These interpolations cause some sharp transitions in the curves of Fig. 7 where the Young's moduli, as predicted by the models, are plotted as a function of composition.

Kolařík had to adjust the critical volume fractions, where it is assumed that co-continuity starts, a posteriori to fit his model to experimental data. As we have an exact knowledge of the range of co-continuity and the morphology at all other compositions, a judicial use of the models for each

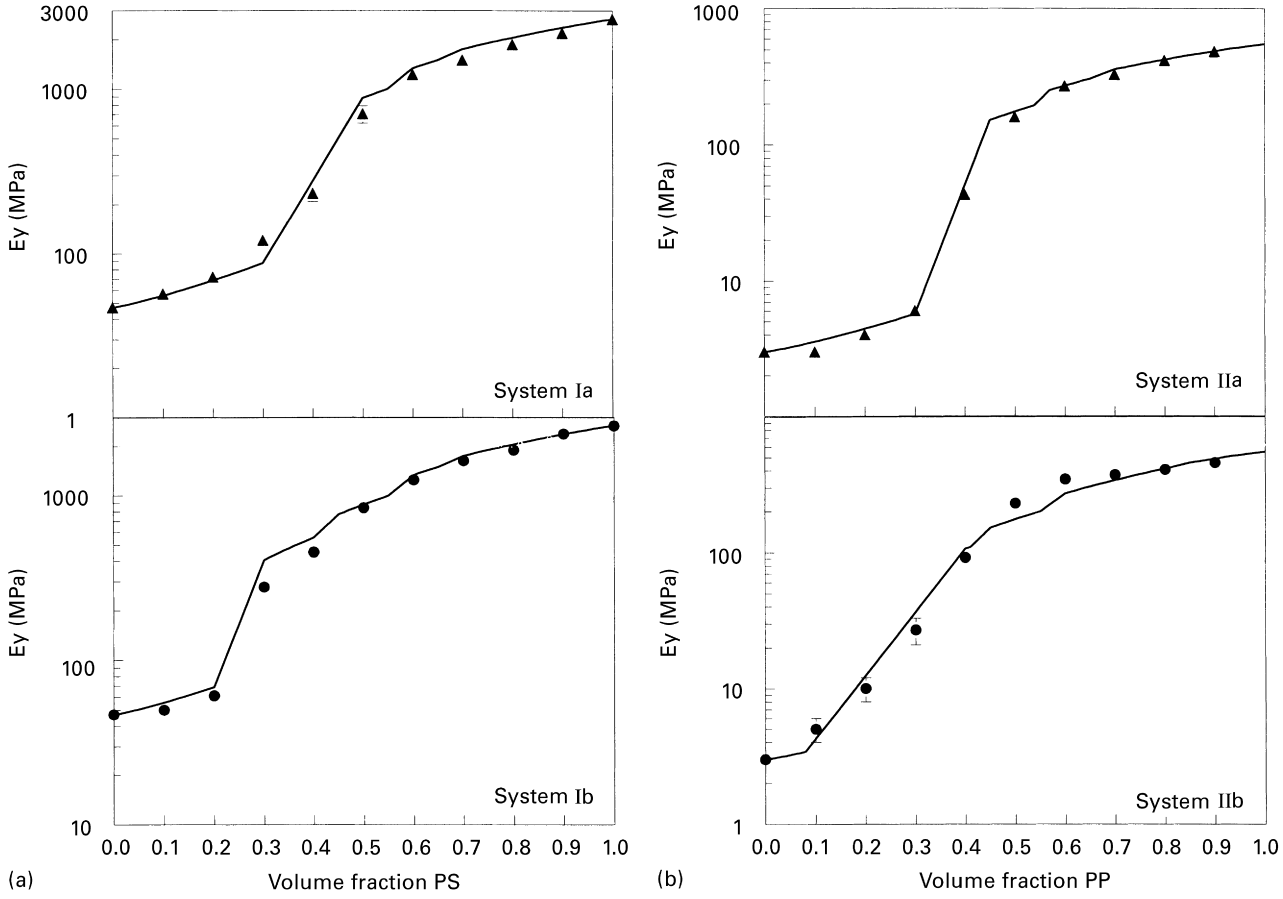

Fig. 7. (a) Young's moduli as function of composition; experimental values for the PS/poly(ether–ester) systems Ia (▲) and Ib (●); (b) Young's moduli as function of composition; experimental values for the PP/SEBS systems IIa (▲) and IIb (●) and predictions (full line) using Eqs. (1)–(4). The judicial use of the equations for each composition range is given in the text.

composition range is possible. For example, for system Ia we used Eq. (2) from 0–30 vol.% PS (stiff droplets in a soft matrix), an average between both the co-continuous models from 50–55 vol.% PS (co-continuous; neither phase dominant), Eq. (3) from 60–65 vol.% PS (co-continuous, stiff phase dominant), and Eq. (1) in the composition range 70–100 vol.% PS (soft droplets in stiff matrix). Linear interpolations, between the various equations, were used in the composition ranges 30–50 vol.% PS (transition from droplet/matrix to co-continuous), 55–60 vol.% PS (transition to stiff phase dominated co-continuity) and 65–70 vol.% PS (transition from co-continuous to droplet/matrix). The results for all four systems can be seen in Fig. 7.

The agreement between the moduli that are predicted by the models and the experimental data is excellent for all systems. This implies that besides the moduli of droplet/matrix blends, the moduli of blends with co-continuous morphologies at all compositions can also be described if only the values of the pure components are known.

In an earlier paper by our group [22], it was shown that the Young's moduli of co-continuous blends of polyethylene (PE) and polystyrene (PS) could not be predicted by the excisting models for co-continuity. Therefore, we compared these earlier results to the models as proposed in Eqs. (3) and (4). Again we used Eq. (4) in the region (35–45 vol.%) where the soft phase dominates, Eq. (3) in the region (50–80 vol.%) where the stiff phase dominates, and an average between both the equations in the intermediate range where neither phase dominates. The linear interpolations result in a stepwise plot as was explained above. The results can be seen in Fig. 8. The agreement between the moduli that are predicted by the models and the experimental data for the co-continuous PE/PS blends is again satisfactory.

4. Conclusions

The elastic moduli of blends with co-continuous morphologies are significantly higher than the moduli of the same blends with a droplet/matrix morphology if the minor phase is the component with the highest modulus, as is demonstrated for poly(ether–ester)/PS and SEBS/PP blends. No significant difference in tensile stress and impact properties are found when co-continuous blends are compared to blends with a dispersed morphology.

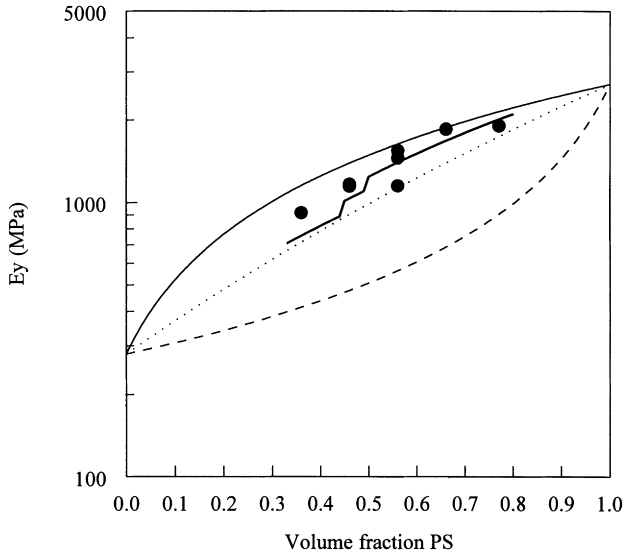

Fig. 8. Young's moduli of co-continuous PE/PS blends (●) and the predictions (full line) using Eqs. (3) and (4). The judicial use of the equations for each composition range is given in the text. For comparison, the parallel (—), series (– – –) and Davies (……) model are shown.

A model is obtained by depicting the co-continuous morphology as three orthogonal bars of the first component embedded in a unit cube where the remaining volume is occupied by the second component, leading to a series model of parallel parts and a parallel model of serial-linked parts. A judicial use of these models results in a perfect description of the moduli of co-continuous blends as a function of composition.

Acknowledgements

The authors would like to thank Ben Norder for help with the DMA experiments and Gerard de Vos for the drawings in Fig. 6 and preparing some DMA samples. Remco C. Willemse is acknowledged for the data points in Fig. 8.

References

[1] Paul DR, Newman S. Polymer blends, 1/2. New York: Academic Press, 1978.
[2] Borggreve RJM, Gaymans RJ, Schuijer J. Polymer 1989;30:71.
[3] van der Sanden MCM. PhD thesis, Eindhoven University of Technology, The Netherlands, 1993.
[4] Joziasse CAP, Topp MDC, Veenstra H, Grijpma DW, Pennings AJ. Polym Bull 1994;33:599.
[5] Verhoogt H, Langelaan HC, van Dam J, Posthuma de Boer A. Polym Engng Sci 1993;33:754.
[6] Machiels AGC, Denys KFJ, van Dam J, Posthuma de Boer A. Polym Engng Sci 1996;36:2451.
[7] Machiels AGC, Denys KFJ, van Dam J, Posthuma de Boer A. Polym Engng Sci 1997;37:59.
[8] Willemse RC, Posthuma de Boer A, van Dam J, Gotsis AD. Polymer 1998;39:5879.
[9] Verhoogt H. PhD thesis, Delft University of Technology, The Netherlands, 1992.
[10] Verhoogt H, van Dam J, Posthuma de Boer A. Adv Chem Ser 1994;239:333.
[11] Veenstra H, van Dam J, Posthuma de Boer A. Polymer 1999;40:1119.
[12] Veenstra H, van Lent BJJ, van Dam J, Posthuma de Boer A. Polymer 1999; in press.
[13] Veenstra H, van Dam J, Posthuma de Boer A. Submitted to Polymer.
[14] Mamat A, Vu-Khanh T, Cigana P, Favis BD. J Polym Sci Part B: Polym Phys 1997;35:2583.
[15] Flexman EA, Huang DD, Snyder HL. Polym Prepr 1988;.
[16] Willemse RC. PhD thesis, Delft University of Technology, The Netherlands, 1998.
[17] Siegfried DL, Thomas DA, Sperling LA. Polym Engng Sci 1981;21:39.
[18] Nishiyama Y, Sperling LH. J Appl Polym Sci 1986;32:5903.
[19] Jordhamo GM, Manson JA, Sperling LH. Polym Engng Sci 1986;26:517.
[20] Ohlsson B, Hassander H, Tornell B. Polym Engng Sci 1996;36:501.
[21] Lyngaae-Jørgenson J, Kuta A, Søndergaard K, Veno Poulson K. Polym Networks Blends 1993;3:1.
[22] Willemse RC, Speijer A, Langeraar AE, Posthuma de Boer A, Polymer, in press.
[23] Gergen WP, Lutz RG, Davison S. In: Legge NR, editor. Thermoplastic elastomers: a comprehensive review, Munich: Hanser, 1986. pp. 507 Chapter 14.
[24] Davies WEA. J Phys D: Appl Phys 1971;4:1325.
[25] Kolařík J. Polym Comp 1997;18:433.
[26] Veenstra H, Hoogvliet RM, Norder B, Posthuma de Boer A. J Polym Sci Part B: Polym Phys 1998;36:1795.
[27] Stricker F, Thomann Y, Mulhaupt R. J Appl Polym Sci 1998;68:1891.
[28] Setz S, Stricker F, Kressler J, Duschek T, Mulhaupt R. J Appl Polym Sci 1996;59:1117.
[29] Takayanagi M, Harima H, Iwata Y. Mem Fac Engng Kyushu Univ 1963;23:41.
[30] Barentsen WM. PhD thesis, Eindhoven University of Technology, The Netherlands, 1972.
[31] Nijhof AHJ. LTM-report 1167, Delft University of Technology, The Netherlands, 1998.